Synthetic and Systems Biotechnology 7 (2022) 965–971

Contents lists available at ScienceDirect

Synthetic and Systems Biotechnology

journal homepage: www.keaipublishing.com/en/journals/synthetic-and-systems-biotechnology

Probing the growth and mechanical properties of *Bacillus subtilis* biofilms through genetic mutation strategies

Suying Liu [a,b,c,1], Jiaofang Huang [d,*,1], Chen Zhang [e], Lihua Wang [f], Chunhai Fan [g], Chao Zhong [c,h,i,**]

[a] Division of Physical Biology and Bioimaging Center, Shanghai Institute of Applied Physics, Chinese Academy of Sciences, Shanghai, China
[b] University of Chinese Academy of Sciences, Beijing, China
[c] School of Physical Science and Technology, ShanghaiTech University, Shanghai, China
[d] State Key Laboratory of Bioreactor Engineering, East China University of Science and Technology, Shanghai, China
[e] Institute of Physics, Swiss Federal Institute of Technology Lausanne (EPFL), Lausanne, Switzerland
[f] The Interdisciplinary Research Center, Shanghai Advanced Research Institute, Chinese Academy of Sciences, Zhangjiang Laboratory, Shanghai, China
[g] School of Chemistry and Chemical Engineering, Institute of Molecular Medicine, Renji Hospital, School of Medicine, Shanghai Jiao Tong University, Shanghai, China
[h] Center for Materials Synthetic Biology, Shenzhen Institute of Synthetic Biology, Shenzhen Institutes of Advanced Technology, Chinese Academy of Sciences, Shenzhen, China
[i] CAS Key Laboratory of Quantitative Engineering Biology, Shenzhen Institute of Synthetic Biology, Shenzhen Institutes of Advanced Technology, Chinese Academy of Sciences, Shenzhen, China

ARTICLE INFO

Keywords:
Bacillus subtilis
Biofilms
Synthetic biology
Living materials
Environmental tolerance

ABSTRACT

Bacterial communities form biofilms on various surfaces by synthesizing a cohesive and protective extracellular matrix, and these biofilms protect microorganisms against harsh environmental conditions. *Bacillus subtilis* is a widely used experimental species, and its biofilms are used as representative models of beneficial biofilms. Specifically, *B. subtilis* biofilms are known to be rich in extracellular polymeric substances (EPS) and other biopolymers such as DNA and proteins like the amyloid protein TasA and the hydrophobic protein BslA. These materials, which form an interconnected, cohesive, three-dimensional polymer network, provide the mechanical stability of biofilms and mediate their adherence to surfaces among other functional contributions. Here, we explored how genetically-encoded components specifically contribute to regulate the growth status, mechanical properties, and antibiotic resistance of *B. subtilis* biofilms, thereby establishing a solid empirical basis for understanding how various genetic engineering efforts are likely to affect the structure and function of biofilms. We noted discrete contributions to biofilm morphology, mechanical properties, and survival from major biofilm components such as EPS, TasA and BslA. For example, EPS plays an important role in maintaining the stability of the mechanical properties and the antibiotic resistance of biofilms, whereas BslA has a significant impact on the resolution that can be obtained for printing applications. This work provides a deeper understanding of the internal interactions of biofilm components through systematic genetic manipulations. It thus not only broadens the application prospects of beneficial biofilms, but also serves as the basis of future strategies for targeting and effectively removing harmful biofilms.

1. Introduction

Bacterial biofilms are bacteria that are embedded in an extracellular matrix of polysaccharides, proteins, nucleic acids, and lipids that provides structural rigidity, protection, and regulation of gene expression and permeability regulation [1–3]. The biofilm is a three-dimensional spatial organization in which molecules interact and communicate with one another, with a tightly packed, heterogeneous

Peer review under responsibility of KeAi Communications Co., Ltd.
* Corresponding author.
** Corresponding author. Center for Materials Synthetic Biology, Shenzhen Institute of Synthetic Biology, Shenzhen Institutes of Advanced Technology, Chinese Academy of Sciences, Shenzhen, China.
E-mail addresses: huangjf@ecust.edu.cn (J. Huang), chao.zhong@siat.ac.cn (C. Zhong).
[1] These two authors contributed equally.

https://doi.org/10.1016/j.synbio.2022.05.005
Received 12 March 2022; Received in revised form 18 May 2022; Accepted 20 May 2022
Available online 3 June 2022

structure [4]. Such biofilms are a major problem in both industry and healthcare [5,6].

Bacillus subtilis is a non-pathogenic Gram-positive bacterium that can form architecturally complex biofilms and is widely used as a model strain for biofilm studies [7,8]. The substrate of *B. subtilis* is similar to other biofilms in that it provides structural rigidity, protects the embedded cells from environmental insults and ensures their presence and propagation [9]. Biofilms are dynamic and can adapt to changing environments [10]. The field of *B. subtilis* biofilm research is rapidly evolving, and some advances have been made in exploring the unique physicochemical properties of biofilms. This includes studies of biofilm wrinkling [11,12], adhesion properties [13–15], and antibiotic resistance [16–19], as well as mechanical properties [20,21]. To expand the uses of biofilms, additional research into the mechanical properties of bacterial biofilms is required.

B. subtilis biofilms are comprised primarily of extracellular polymeric substances (EPS) and the amyloid protein TasA and the hydrophobic protein BslA (Fig. 1). EPS contributes to the formation of biofilm structure, helps biofilm to adhere to the surface and provides mechanical stability to the biofilm [22–24]. TasA polymerizes into highly stable amyloid fibers, which serve as the biofilm's structural "backbone" and are involved in the formation of the biofilm matrix [25–29]. BslA forms a hydrophobic layer on the surface of the biofilm, which may contribute to its resistance to antimicrobials and disinfectants [30,31]. The morphology, internal structure, and mechanical stability of biofilms are heavily influenced by the polymers that comprise them. In this study, we investigated the effect of EPS, TasA and BslA, the main components of *B. subtilis* biofilms, on the mechanical properties. We genetically engineered various mutant strains to test their growth state, mechanical properties, antibiotic tolerance, and printing ability. Biofilms are cross-linked polymer gel composites that can be three-dimensional (3D) printed as bioinks [32]. Previous study used engineered *B. subtilis* biofilms to demonstrate a programmable and printable platform of living functional materials [33]. Based on this research, we can select host bacteria that are more suitable for printing and use functional 3D printed biofilms to construct living biofilm-derived materials, which may have broad applications in the future.

2. Materials and methods

2.1. Strains and plasmids

Bacillus subtilis 2569 wild-type (WT, Kind gift from Daniel Kearns) was employed, and mutant strains were constructed and sequenced including *tasA* mutant (ΔtasA), *epsÃ O* mutant (Δeps), *bslA* mutant (ΔbslA), *tasA*, *epsÃ O* and *bslA* mutant (ΔtasAΔepsΔbslA). Peptide insert regions were either fully synthesized (Genewiz, China) or PCR-generated overlap extension. All cloning was performed using molecular cloning and isothermal Gibson Assembly, and verified by DNA sequencing. Detailed information about the construction of genes and strains were described in Tables S1 and S2.

2.2. Strain construction

The biofilm-defective strains ΔtasA, Δeps, ΔbslA and ΔtasAΔepsΔbslA were constructed following the same protocol. Here, we used the ΔtasA strain construction as an example to describe the specific protocol. Specifically, the fusion fragment was created by amplifying gene fragments upstream and downstream of *tasA* with primer pairs pMAD-ΔtasAF1/pMAD-ΔtasAR1 and pMAD-ΔtasAF2/pMAD-ΔtasAR2. Then inserting the fusion fragment into the pMAD plasmid to obtain the suicide plasmid pMAD-ΔtasA. After that, transforming pMAD-ΔtasA into *B. subtilis* WT cell, and screening test of resistance to erythromycin. PCR fragments from mutant genomic DNA were sequenced to confirm the deletions of *tasA*. Detailed information about the construction of primers were described in Table S3.

2.3. General condition for biofilm growth

MSgg broth: 100 mM morpholinepropane sulphonic acid (Mops) (pH 7), 0.5% glycerol, 0.5% glutamate, 5 mM potassium phosphate (pH 7), 50 μg/mL tryptophan, 50 μg/mL phenylalanine, 2 mM$MgCl_2$, 700 μM$CaCl_2$, 50 μM$FeCl_3$, 50 μM$MnCl_2$, 2 μM thiamine, 1 μM $ZnCl_2$.

Liquid cultured biofilms: Seed cultures were grown in LB-Miller medium for 12 h at 37 °C, with shaking at 220 rpm. Then the bacteria were harvested and resuspended in MSgg medium (OD = 1), biofilm cultures were grown at 30 °C for 2–3 days.

Solid cultured biofilms: Seed cultures were grown in LB-Miller medium for 12 h at 37 °C, with shaking at 220 rpm. Then the bacteria were harvested and resuspended in MSgg medium (OD = 1), the suspension was dripped on the 1.5% agar MSgg medium, and biofilm cultures were grown at 30 °C for 2–3 days.

2.4. Water contact angle

A drop of 10 μl of water was loaded to the surface of biofilm on MSgg agar plate, and the contact angle of these biofilms was then measured at room temperature using a Theta Lite optical tensiometer (Biolin).

2.5. Transmission electron microscopy (TEM)

To prepare the samples we used carbon-coated grids (Zhongjingkeyi

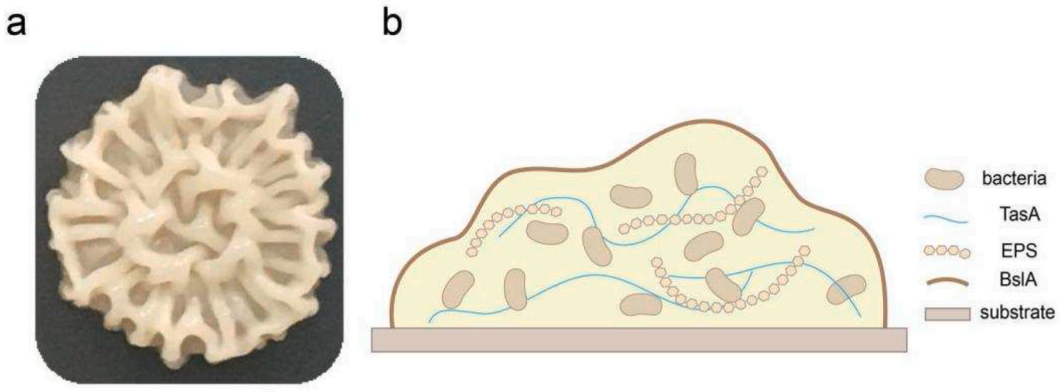

Fig. 1. *Bacillus subtilis* biofilms formation. (**a**) Digital camera image of the wild-type *B. subtilis* biofilm. The mature biofilm exhibits a complex network of intertwined wrinkles and ridges and is highly hydrophobic. (**b**) A schematic of wild-type *B. subtilis* biofilm. The biofilm matrix composition is complex and can contain self-produced molecules, including TasA fibers, EPS, BslA and bacteria.

Technology, EM Sciences) that were placed on top of a 20 μl drop of liquid culture for 1–5 min. The grid was washed by PBS buffer and water, and the excess liquid was blotted off on a filter paper (Whatman no. 1) and negatively stained with uranyl acetate (1–2% aqueous solution). The samples were dried and examined in a JSM 1400 transmission electron microscope at an accelerating voltage of 120 kV.

2.6. Scanning electron microscopy (SEM)

Biofilm samples were directly dropped onto sterile aluminized paper, washed with millipore H_2O and fixed with 2% glutaraldehyde and 2% paraformaldehyde, then washed again with millipore H_2O, and dehydrated with an increasing ethanol step gradient. Then aluminized paper samples were stuck onto a specimen holder and sputter coated with gold, and finally imaged with a JEOL JSM-7800 scanning electron microscope operated at 5 kV accelerating voltage.

2.7. Antibiotic resistance

Seed cultures were grown in LB-Miller medium for 12 h at 37 °C, with shaking at 220 rpm. Then the bacteria were harvested and resuspended in MSgg medium (OD = 1), the suspension was dripped on the 1.5% agar MSgg medium containing different concentrations of chloramphenicol, and biofilm cultures were grown at 30 °C for 2–3 days. Then collected the biofilms and measured their biomass.

2.8. Rheology measurement

Rheological experiments were performed on a strain-controlled rheometer (Anton paar MCR101) equipped with a 24.948 mm diameter cone plate. All biofilm samples were scraped from an MSgg plate and placed on the cone plate. The samples were surrounded with water to minimize evaporation. The tested gap height was set as 0.048 mm. Strain sweep experiments from 0.01% to 10% strain amplitude was performed at 10 rad/s to determine the linear viscoelastic region. Frequency sweep experiments from 100 to 0.01 rad/s were performed at 1% strain amplitude. The temperature was maintained at 25 °C by a thermoelectric device.

2.9. 3D printing

Biofilms were scraped off the MSgg plates and placed into the charging barrels of a robotic 3D printer (GeSim BioScaffolder 3.1). The shapes of polygons or circles were printed using the existing graph program in the system. The printing parameters applied in the experiments were: printing pressure (250 kPa), the inner diameter of the nozzle (160 μm), and printing speed (5 mm/s).

3. Results

3.1. Macroscopic and microscopic structure of liquid cultured biofilm-defective strains

Based on the *B. subtilis* 2569 wild-type strain (WT), we constructed mutant strains of biofilm-relevant genes knockout as follows: *tasA* mutant (ΔtasA), *epsÃ O* mutant (Δeps), *bslA* mutant (ΔbslA), and a triple knockout *tasA*, *epsÃ O*, and *bslA* mutant (ΔtasAΔepsΔbslA). The mechanical properties of a biofilm can be influenced by both its micro- and macrostructure. We compared 2-day solid cultured WT and mutant biofilms and observed their morphology with a light microscope and electron microscopes, respectively. The WT biofilm shows a typical pellicle, while all mutant strains are impaired in biofilm formation and form flat, fragile pellicles (Fig. 2a and Fig. S1). Employing field emission scanning electron microscopy (SEM, Fig. 2b) and transmission electron microscopy (TEM, Fig. 2c), fibers were observed in WT, Δeps, and ΔbslA pellicles, but not in ΔtasA or ΔtasAΔepsΔbslA pellicles (Fig. 2c), suggesting that the observed fibers were mainly composed of TasA proteins. We also used water contact angle experiments to assess the

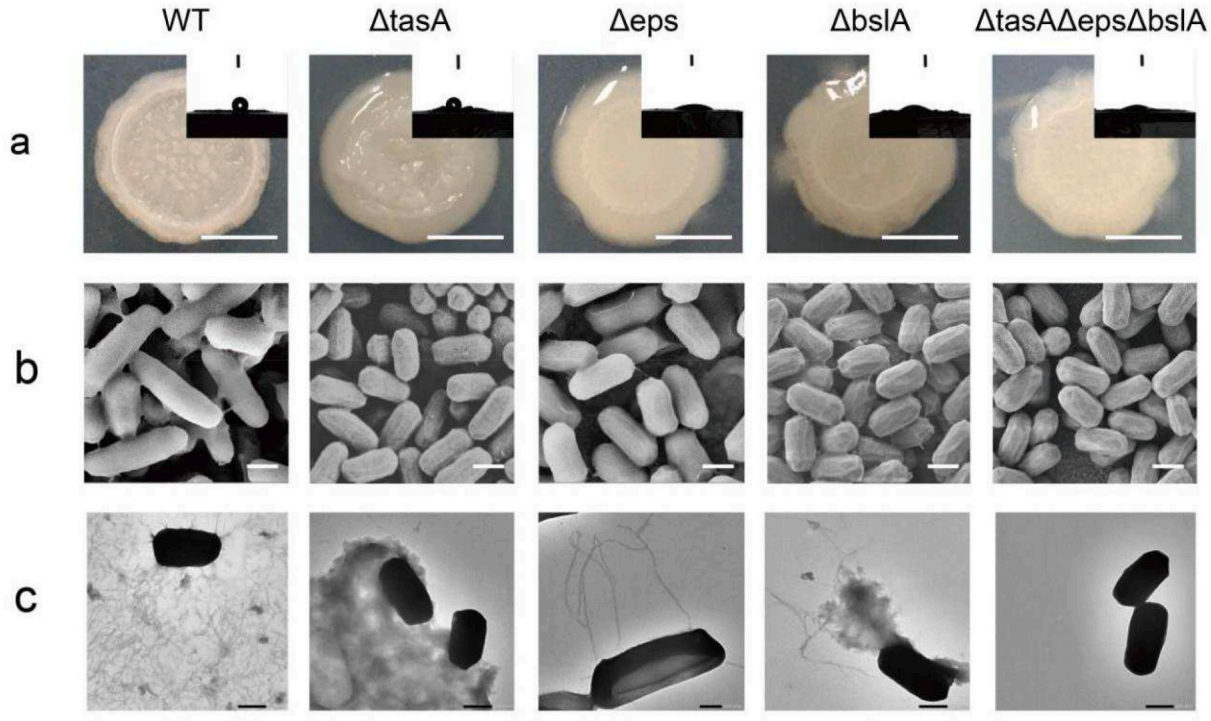

Fig. 2. Macroscopic and microscopic structure of *B. subtilis* biofilms. (a) Digital camera image of WT, single mutant, and multiple knockout *B. subtilis* biofilms. Water contact assay was also shown (insets). WT biofilm had a typical wrinkled pellicle that exhibits strong hydrophobicity. Microscale observations including (b) FE-SEM and (c) TEM. There was no amyloid fiber in the *tasA* knockout sample, no extracellular polysaccharide in the *epsÃ O* knockout sample, and no extracellular matrix in the triple knockout sample. Note: all the biofilms used in the above experiments were cultured for two days. Scale bar: 5 mm in a, 500 nm in b and c.

hydrophobicity of biofilms. The WT biofilm and the ΔtasA biofilm were both extremely hydrophobic. In contrast, the Δeps and ΔbslA as well as the ΔtasAΔepsΔbslA biofilm demonstrated very strong hydrophilic properties (Fig. 2a, insert). The results imply that, compared to both the EPS and BslA components, the TasA proteins may not significantly contribute to the hydrophobicity of the biofilms. The phenotype of the ΔbslA pellicle supports previous findings that in addition to contributing to liquid repellency, the assembly of BslA layers may confer structural stability to the biofilm matrix and enable the biofilm matrix to maintain sufficient 'space' for gas retention [34].

3.2. Growth curves and antibiotic resistance of *B. subtilis* biofilms

We next measured the dynamic growth, as indicated by the biomass as a function of growth time, during biofilm development over a 6-day culture (Fig. 3a). The fact that the ΔtasA is the slowest, combined with the observation that the triple mutant, which also lacks the TasA protein, ranks second worst, clearly indicates the important of TasA in biofilm growth. Group differences in the water contact angle (WCA; Fig. 3b) confirmed our results from the water contact assay (Fig. 2a) which showed that the WT and ΔtasA biofilms had hydrophobic properties while the Δeps, ΔbslA, and ΔtasAΔepsΔbslA biofilms had hydrophilic properties. During the six-day culture, the contact angle of each biofilm had barely changed (Fig. 3b). Weight measurements demonstrated that almost all of the mutant biofilms exhibited development retardation by day 5 (Fig. 3c). And the ΔtasA biofilm had the slowest growth rate and the least biomass. In addition, antibiotic resistance testing with chloramphenicol, morphological observation, and biofilm biomass determination was performed after 2 days culture at 30° (Fig. 3d). The Δeps biofilm exhibited a significantly lower biomass than other single mutant biofilm, demonstrating that EPS contribute to antibiotic resistance (Fig. 3e). This observation implied that EPS constitutes a significant component of biofilm and effectively prevents the entry of antibiotics into cells. Moreover, it is conceivable that EPS may alter the antibiotic resistance of the biofilm by altering the water content and osmotic pressure of the biofilm, as penetrating more slowly may allow time for an adaptive phenotypic response that could potentially improve tolerance [35,36].

3.3. Physiochemical and mechanical properties of *B. subtilis* biofilms

We next investigated the rheological properties of WT and mutant biofilms. Fig. 4a showed the change in viscosity of the different biofilms. The WT biofilm exhibited a relatively high viscosity compared to mutant biofilms. The biofilms exhibited shear-thinning behavior and the viscosity decreased with increasing shear rate. The oscillatory shear stress scans revealed that the biofilms all exhibited predominantly viscous behavior (Fig. 4b). The gel-like nature of the samples can be analyzed by the dependence of the storage modulus G′ and loss modulus G″ on the angular frequency ω. $G' > G''$ with the change in angular frequency was found for all biofilm samples (Fig. 4c), indicating that all biofilms had a gel-like structure. Several precise test conditions were set up to quantify the biofilms' viscosity and flexibility. However, the mechanical strength of the WT biofilm in the present work was much weaker compared to previously published work. We speculate that these bacteria underwent internal changes during several years of self-transfer and replication in the laboratory. Furthermore, laboratory factors such as air humidity and temperature might alter the water content of the biofilm, resulting in discrepancies in the results. Of course, we believe that the results of the rheological tests in this paper are still relevant because they were performed under the same conditions and with the same batch of strains. The shear viscosity of the biofilms was measured at a selected shear rate

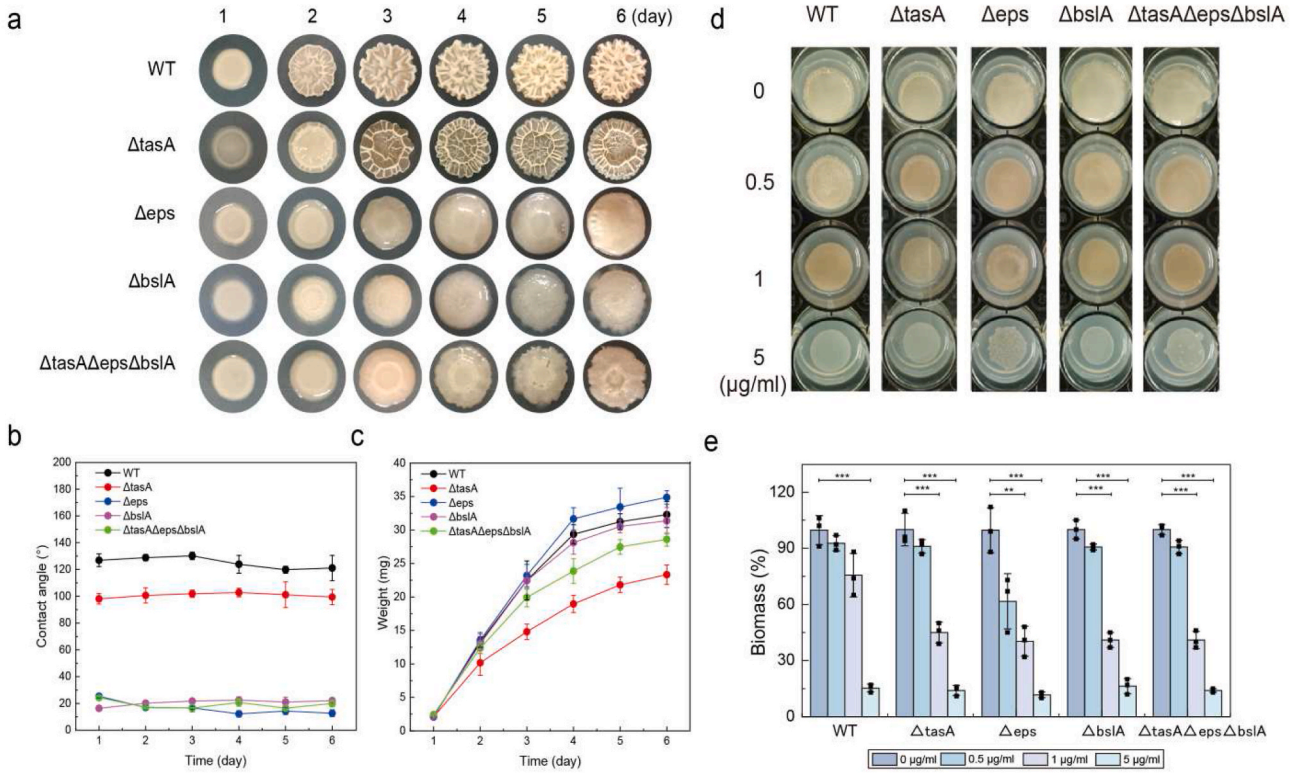

Fig. 3. Growth status and antibiotic resistance of *B. subtilis* biofilms. (a) The growth status of WT and mutant *B. subtilis* biofilms over a 6-day culture. (b) Water contact angle and (c) weight of WT and mutant *B. subtilis* biofilms. (d) Antibiotic resistance of solid cultured biofilms. (e) Biomass of biofilms in solid cultured with different concentrations of chloramphenicol. The ΔEPS biofilm exhibited a significantly lower biomass than other single mutant biofilm, demonstrating that EPS contributed to antibiotic resistance. Note: each of the circles in a has a diameter of 1.25 cm. Experiments in b, c and e were repeated three times with similar results based on biologically independent biofilm cultures (n = 3). Experiments in e were repeated three times (n = 3). **P < 0.01, ***P < 0.001, two-sided *t*-test.

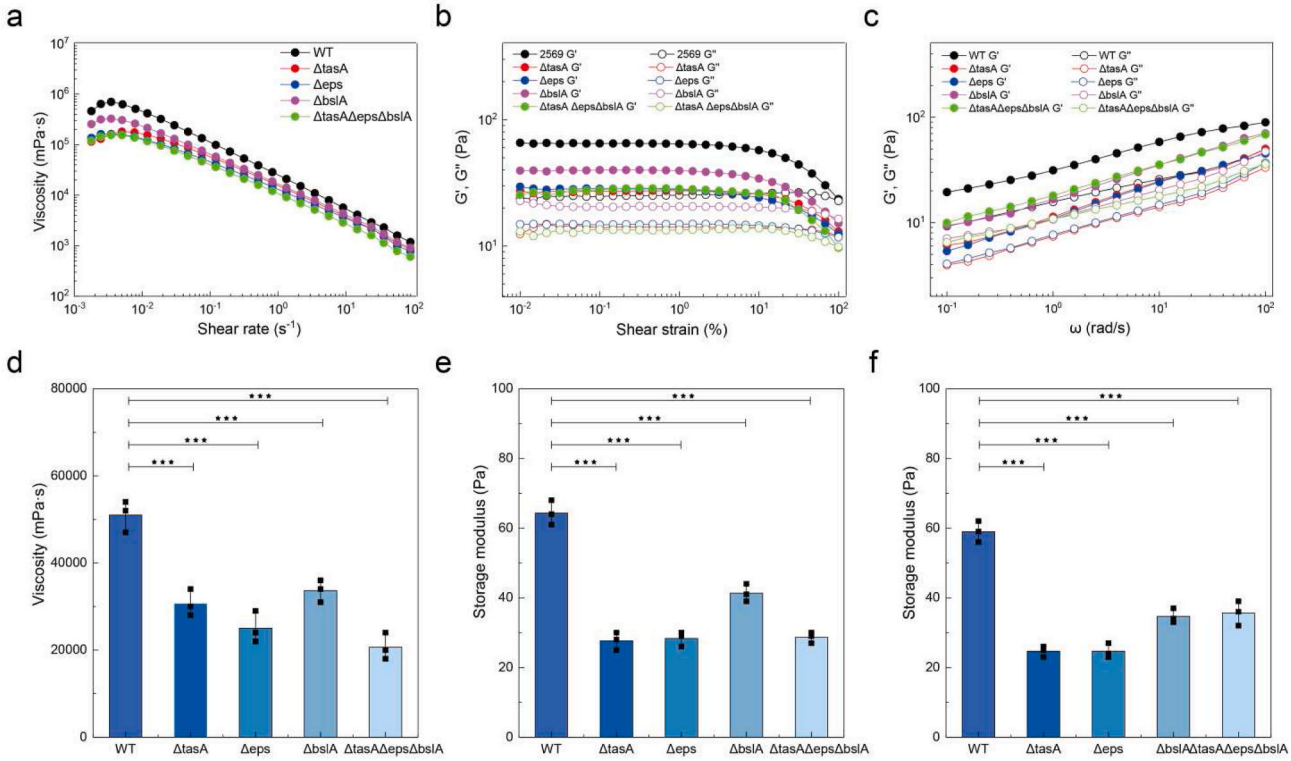

Fig. 4. Rheological properties of *B. subtilis* biofilms. (a) The steady-state flow behavior of biofilms measured by viscosity curves at changing shear rates (from 0.001 to 100 s-1). The biofilms exhibited shear-thinning behavior. (b) The measured storage modulus (G′) and loss modulus (G″) of different biofilm variants as a function of strain amplitude from 0.01 to 100% angular frequency, 1 rad/s. The biofilms all exhibited predominantly viscous behavior. (c) The measured storage modulus (G′) and loss modulus (G″) of different biofilm variants as a function of angular frequency from 0.1 to 100 rad/s (strain amplitude, 1%). All biofilms had a gel-like structure. (d) Shear viscosity of biofilms at a selected shear rate of 0.316 s–1. (e) Storage modulus of biofilms at a selected strain amplitude of 1%. (f) Storage modulus of biofilms at a selected angular frequency of 10 rad/s. The WT biofilm exhibited relatively strong viscoelasticity. All experiments were repeated three times (n = 3). ***P < 0.001, two-sided *t*-test.

of 0.316 s^{-1} (Fig. 4d). The storage modulus of the biofilms was measured at a selected strain amplitude of 1% (Fig. 4e) and at a selected angular frequency of 10 rad/s (Fig. 4f), respectively. In the above experiments, the WT biofilm exhibited relatively stronger viscoelasticity. TasA served as the structural "backbone" of the biofilm, on which the more flexible and amorphous EPS was superimposed. As a result of the stent effect, the TasA amyloid fibers might provide stiffness to the biofilm [37,38]. In the three-dimensional structure of biofilms, EPS along with other substances impacted the growth of biofilms [39]. The BslA was a hydrophobic layer on the biofilm's outer surface, and its absence made the biofilm less resistant and softer overall. In addition, these results indicated that both EPS and BslA contribute to the elasticity of biofilms.

3.4. 3D printing of B. subtilis biofilms

As *B. subtilis* biofilms exhibit typical hydrogel behaviors, we next evaluated the 3D printing characteristics of WT and mutant biofilms using our previously developed 3D printing platform. The rheological properties of biofilms had a significant impact on the physical stability of the high-precision 3D printed structures. We printed regular pentagon shapes using the WT and mutant biofilms with the same printing conditions (nozzle diameter set to 90 μm), the lines of the WT biofilm were substantially expanded compared to the mutant biofilms (Fig. 5a and Fig. S4). Rheological measurements and comparisons of the storage modulus (G', representing elastic deformation) suggested that the relatively high viscoelasticity of the WT biofilms made them less suitable for printing (Fig. 4a, c, e). In addition, to simulate printing conditions, a sudden shear process in a steady state (100 s−1), followed by an oscillatory sweep measurement were applied to WT and mutant biofilms (Fig. 5b). All the biofilms showed an immediate recovery in viscosity even after multiple cycles. The extent of biofilm viscosity recovery was then measured (Fig. 5c). Among the mutant strains, the viscoelastic network of ΔbslA had the strongest instantaneous recovery capability. Similarly, in printing, the deformation of biofilms was minimized, making them more suitable for 3D printing. Collectively, the result implicated that we could tune the resolution of printed biofilms by genetically altering the extra-cellular components.

4. Discussion

Previous efforts have attempted to explore *B. subtilis* biofilm formation. Focusing on the physical properties of *B. subtilis* biofilms as in the case of this study, many of these mathematical and experimental investigations analyzed the influence of three key biofilm matrix components on the biofilm colonies. Kesel et al. quantitatively investigated the surface roughness, stiffness and the bulk viscoelasticity of biofilms and demonstrated the importance of specific biofilm matrix components for the distinct physical properties and biofilm growth of *B. subtilis* biofilms [40,41]. Benigar et al. reported on the structure and dynamics of biologically important model polymer mixtures that mimic the extracellular polymeric matrix in native biofilm of *Bacillus subtilis* [42]. In addition, a combined experimental and computational approach had been applied to investigate potential benefits arising from division of labor during biofilm matrix production [43]. Previous studies suggested that there is an internal force within the biofilm that helps it to shape its structure, improves the mechanical resistance, and facilitates its invasion and self-repair [44]. Yannarell et al. explored a striking dual-species biofilm [45]. Klotz et al. quantified the impact of specific biofilm matrix components on biofilm erosion behavior [46]. Despite those advances, it still lacks a whole picture regarding how specific biofilm components

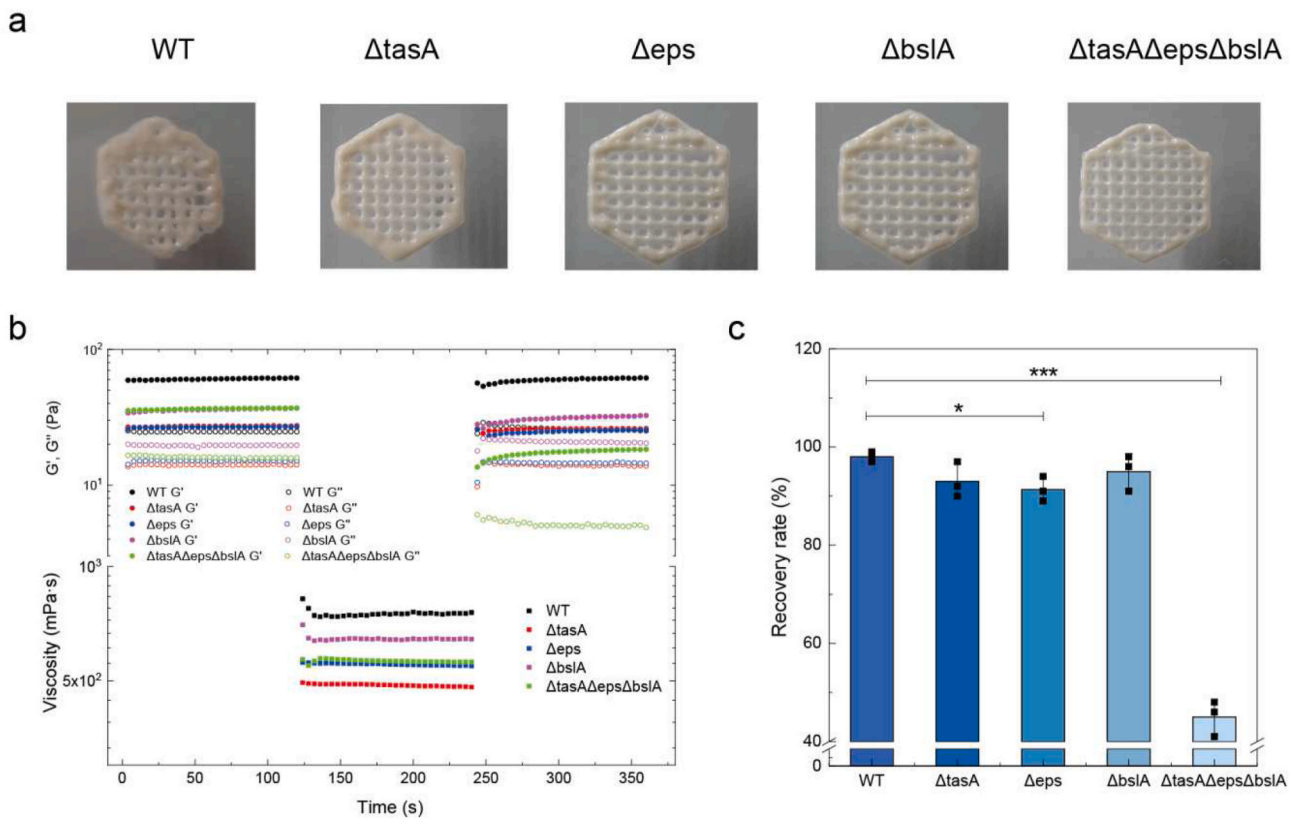

Fig. 5. Printability of *B. subtilis* biofilms. (a) Digital images of 3D printed *B. subtilis* biofilm variants. The printed lines of the WT biofilm were substantially expanded compared to the mutant biofilms. (b) Instantaneous recovery of the viscoelastic network of biofilms shown by a sudden shear process in a steady state (100 s^{-1}), followed by an oscillatory sweep measurement. All the biofilms showed an immediate recovery in viscosity. (c) The extents of viscosity recovery of biofilm variants were measured (t1 = 60 s, t2 = 300 s). The ΔbslA biofilm had the strongest instantaneous recovery capability among other mutant biofilms. Experiments in b and c were repeated three times (n = 3). *P < 0.05, ***P < 0.001, two-sided *t*-test.

affect the structures, mechanical and biological properties of biofilms.

In this study, using *B. subtilis* as a model system, we looked into how specific biofilm components affect macroscopic and microscopic structures, as well as properties like stiffness and printability. We were mainly interested in how biofilm-relevant genes influence the physical and growth properties of *B. subtilis* during biofilm formation. Understanding the basic components underlying the mechanical properties of biofilms, as well as the effects of various external stresses affected the biofilms, can be a valuable strategy for gaining structural insights. The application of a combination of genotype and phenotype approaches, as well as quantitatively determining the influence of its individual constituents on biofilm structure, mechanics, and permeability, might be the most promising way to achieve the goal of dissecting the relationship between the molecular composition of a biofilm and its properties. A thorough understanding of biofilm compositions should enable us to control biofilm formation in the future, potentially easing biofilm removal. Biofilms with specific properties might be used as engineered living materials (ELMs) for biomedical applications [47].

The altered matrix gene expression patterns in ΔtasA suggested that a higher proportion of TasA might be required for stable pellicle production. The outward expansion during biofilm growth is limited by the surface layer protein BslA encapsulating the biofilm, and the area covered by the biofilm is slightly increased in the presence of EPS. In the case of EPS, it can simply increase the biomass and thus increase the total coverage of the biofilm. The knockout strain showed weaker mechanical properties compared to the wild strain, indicating that the material properties of the biofilm may vary depending on the important components of the biofilm. The information regarding how biofilm components affect the properties of biofilms can be used a reference for combating bacterial biofilms on medical devices or industrial surfaces in the future. In addition, living materials with unprecedented functionalities can be created using the freedom of shape provided by this printing technique and the inherent performance of biofilm [48–50].

Credit author statement

C. Zhong and J.F.H directed the research; S.Y.L, J.F.H and C. Zhong conceived of the idea and designed the research. J.F.H. constructed mutants and cultured biofilms. S.Y.L., J.F.H. and C. Zhang did the electron microscopy experiments and rheological measurements. S.Y.L. did 3D printing and antibiotic resistance. S.Y.L., J.F.H., and C. Zhong analyzed the data, discussed results, and wrote the manuscript, with the help from L.H.W and C.H.F.

Declaration of competing interest

There are no conflicts to declare.

Acknowledgements

SEM and TEM characterization was performed at the ShanghaiTech EM Center, Shanghai. This work was partially funded by the National Key R&D Program of China (Nos. 2020YFA0908100 and 2021YFA0910800), the National Science Fund for Distinguished Young Scholars (No. 32125023) for C. Zhong, and partially supported by grants from the National Natural Science Foundation of China (No.31872728), the National Science and Technology Major Project of the Ministry of Science and Technology of China (2020YFA0908900) and the Science and Technology Commission of Shanghai Municipality (Nos. 19ZR1477100 and 22ZR1416000) for J. F. Huang.

Appendix A. Supplementary data

Supplementary data to this article can be found online at https://doi.org/10.1016/j.synbio.2022.05.005.

References

[1] Lopez D, Vlamakis H, Kolter R. *Biofilms.* Cold Spring Harb Perspect Biol 2010;2(7):a000398.
[2] Flemming HC, et al. Biofilms: an emergent form of bacterial life. Nat Rev Microbiol 2016;14(9):563–75.
[3] Hobley L, et al. Giving structure to the biofilm matrix: an overview of individual strategies and emerging common themes. FEMS Microbiol Rev 2015;39(5):649–69.
[4] Flemming HC, Wingender J. The biofilm matrix. Nat Rev Microbiol 2010;8(9):623–33.
[5] Hall-Stoodley L, Costerton JW, Stoodley P. Bacterial biofilms: from the natural environment to infectious diseases. Nat Rev Microbiol 2004;2(2):95–108.
[6] Penesyan A, Gillings M, Paulsen IT. Antibiotic discovery: combatting bacterial resistance in cells and in biofilm communities. Molecules 2015;20(4):5286–98.
[7] Arnaouteli S, et al. Bacillus subtilis biofilm formation and social interactions. Nat Rev Microbiol 2021;19(9):600–14.
[8] Si T, et al. Characterization of Bacillus subtilis colony biofilms via mass spectrometry and fluorescence imaging. J Proteome Res 2016;15(6):1955–62.
[9] Dragos A, et al. Evolution of exploitative interactions during diversification in Bacillus subtilis biofilms. FEMS Microbiol Ecol 2017;93(12).
[10] Wilking JN, A TE, Seminara A, et al. Biofilms as complex fluids. MRS Bull 2011;36(5):385–91.
[11] Tan Y, et al. Bioinspired multiscale wrinkling patterns on curved substrates: an overview. Nano-Micro Lett 2020;12(1):101.
[12] Trejo M, et al. Elasticity and wrinkled morphology of Bacillus subtilis pellicles. Proc Natl Acad Sci U S A 2013;110(6):2011–6.
[13] Charlton SGV, et al. Regulating, measuring, and modeling the viscoelasticity of bacterial biofilms. J Bacteriol 2019;201(18).
[14] Kretschmer M, Schussler CA, Lieleg O. Biofilm adhesion to surfaces is modulated by biofilm wettability and stiffness. Adv Mater Interfac 2021;8(5):2001658.
[15] Zhang C, et al. Engineered Bacillus subtilis biofilms as living glues. Mater Today 2019;28:40–8.
[16] Yen P, Papin JA. History of antibiotic adaptation influences microbial evolutionary dynamics during subsequent treatment. PLoS Biol 2017;15(8):e2001586.
[17] Epstein AK, et al. Bacterial biofilm shows persistent resistance to liquid wetting and gas penetration. Proc Natl Acad Sci U S A 2011;108(3):995–1000.
[18] Camara-Almiron J, et al. Dual functionality of the amyloid protein TasA in Bacillus physiology and fitness on the phylloplane. Nat Commun 2020;11(1):1859.
[19] Hall CW, Mah TF. Molecular mechanisms of biofilm-based antibiotic resistance and tolerance in pathogenic bacteria. FEMS Microbiol Rev 2017;41(3):276–301.
[20] Hollenbeck EC, et al. Mechanical behavior of a Bacillus subtilis pellicle. J Phys Chem B 2016;120(26):6080–8.
[21] Tallawi M, Opitz M, Lieleg O. Modulation of the mechanical properties of bacterial biofilms in response to environmental challenges. Biomater Sci 2017;5(5):887–900.
[22] Flemming HC, Neu TR, Wozniak DJ. The EPS matrix: the "house of biofilm cells". J Bacteriol 2007;189(22):7945–7.
[23] Ido N, et al. Bacillus subtilis biofilms characterized as hydrogels. Insights on water uptake and water binding in biofilms. Soft Matter 2020;16(26):6180–90.
[24] Frances, et al. A novel regulatory protein governing biofilm formation in Bacillus subtilis. Mol Microbiol 2008;68(5):1117–27.
[25] Taglialegna A LI, Valle J. Amyloid structures as biofilm matrix scaffolds. J Bacteriol 2016;198(19):2579–88.
[26] Romero D AC, Losick R, et al. Amyloid fibers provide structural integrity to Bacillus subtilis biofilms. Proc Natl Acad Sci Unit States Am 2010;107(5):2230–4.
[27] Earl C, et al. The majority of the matrix protein TapA is dispensable for Bacillus subtilis colony biofilm architecture. Mol Microbiol 2020;114(6):920–33.
[28] Stover AG, Driks A. Secretion, localization, and antibacterial activity of TasA, a Bacillus subtilis spore-associated protein. J Bacteriol 1999;181(5):1664–72.
[29] Branda SS, et al. A major protein component of the Bacillus subtilis biofilm matrix. Mol Microbiol 2006;59(4):1229–38.
[30] Vlamakis H, et al. Sticking together: building a biofilm the Bacillus subtilis way. Nat Rev Microbiol 2013;11(3):157–68.
[31] Kobayashi K, Iwano M. BslA(YuaB) forms a hydrophobic layer on the surface of Bacillus subtilis biofilms. Mol Microbiol 2012;85(1):51–66.
[32] Balasubramanian S, Aubin-Tam ME, Meyer AS. 3D printing for the fabrication of biofilm-based functional living materials. ACS Synth Biol 2019;8(7):1564–7.
[33] Huang J, et al. Programmable and printable Bacillus subtilis biofilms as engineered living materials. Nat Chem Biol 2019;15(1):34–41.
[34] Hobley L, et al. BslA is a self-assembling bacterial hydrophobin that coats the Bacillus subtilis biofilm. Proc Natl Acad Sci U S A 2013;110(33):13600–5.
[35] Walters 3rd MC, et al. Contributions of antibiotic penetration, oxygen limitation, and low metabolic activity to tolerance of Pseudomonas aeruginosa biofilms to ciprofloxacin and tobramycin. Antimicrob Agents Chemother 2003;47(1):317–23.
[36] Cairns LS, Hobley L, Stanley-Wall NR. Biofilm formation by Bacillus subtilis: new insights into regulatory strategies and assembly mechanisms. Mol Microbiol 2014;93(4):587–98.
[37] Diehl A, et al. Structural changes of TasA in biofilm formation of Bacillus subtilis. Proc Natl Acad Sci U S A 2018;115(13):3237–42.
[38] Otto SB, et al. Privatization of biofilm matrix in structurally heterogeneous biofilms. mSystems 2020;5(4):e00425-20.
[39] Peng N, et al. The exopolysaccharide-eDNA interaction modulates 3D architecture of Bacillus subtilis biofilm. BMC Microbiol 2020;20(1):115.
[40] Kesel S, et al. Direct comparison of physical properties of Bacillus subtilis NCIB 3610 and B-1 biofilms. Appl Environ Microbiol 2016;82(8):2424–32.
[41] Kesel S, et al. Matrix composition determines the dimensions of Bacillus subtilis NCIB 3610 biofilm colonies grown on LB agar. RSC Adv 2017;7(51):31886–98.
[42] Benigar E, et al. Structure and dynamics of a model polymer mixture mimicking a levan-based bacterial biofilm of Bacillus subtilis. Langmuir 2016;32(32):8182–94.
[43] Dragos A, et al. Division of labor during biofilm matrix production. Curr Biol 2018;28(12):1903–13. e5.
[44] Douarche C, Allain JM, Raspaud E. Bacillus subtilis bacteria generate an internal mechanical force within a biofilm. Biophys J 2015;109(10):2195–202.
[45] Yannarell SM, et al. A dual-species biofilm with emergent mechanical and protective properties. J Bacteriol 2019;201(18):e00670-18.
[46] Klotz M, et al. Importance of the biofilm matrix for the erosion stability of Bacillus subtilis NCIB 3610 biofilms. RSC Adv 2019;9(20):11521–9.
[47] Konkol MA, Blair KM, Kearns DB. Plasmid-encoded ComI inhibits competence in the ancestral 3610 strain of Bacillus subtilis. J Bacteriol 2013;195(18):4085–93.
[48] Schmieden DT, Basalo Vázquez SJ, Sangüesa H, van der Does M, Idema T, Meyer AS. Printing of patterned, engineered E. coli biofilms with a low-cost 3D printer. ACS Synthetic Biol. 2018;7(5):1328–37.
[49] Balasubramanian S, et al. Emergent biological endurance depends on extracellular matrix composition of three-dimensionally printed Escherichia coli biofilms, 10; 2021. p. 2997–3008. 11.
[50] Dubbin K, et al. Projection microstereolithographic microbial bioprinting for engineered biofilms. Nano Lett 2021;21(3):1352–9.